Available online at www.sciencedirect.com
ScienceDirect
Advances in Space Research 41 (2008) 1773–1783
ADVANCES IN SPACE RESEARCH (a COSPAR publication)
www.elsevier.com/locate/asr

An automatic procedure to identify key vegetation phenology events using the JRC-FAPAR products

Michel M. Verstraete *, Nadine Gobron, Ophélie Aussedat, Monica Robustelli, Bernard Pinty, Jean-Luc Widlowski, Malcolm Taberner

European Commission – DG Joint Research Centre, Institute for Environment and Sustainability, TP 440, I-21020 Ispra (VA), Italy

Received 27 October 2006; received in revised form 23 May 2007; accepted 24 May 2007

Abstract

The phenology of vegetation, which describes the seasonal evolution of plants, can be effectively monitored from space. This approach offers important advantages compared to field observations, as quantitative information can be derived for any location worldwide over a number of years, thereby offering a consistent overview of the fate of the observed biomes and their relations with the climate and the environment. This manuscript describes a method to define the start, end, and length of 'growing seasons' based on the statistical analysis of time series of the biogeophysical quantity known as the Fraction of Absorbed Photosynthetically Active Radiation derived from an analysis of SeaWiFS data. Results are discussed for various biomes.
© 2007 COSPAR. Published by Elsevier Ltd. All rights reserved.

Keywords: Earth observation; FAPAR; Growing season; Phenology; Remote sensing; Sigmoid; Terrestrial environments

1. Introduction

One of the most conspicuous and critical characteristics of vegetation is its seasonal variability. In most locations, the plant cover tends to grow and develop, then senesce and possibly die down on an annual basis. This seasonal evolution results from natural and human-induced constraints such as the availability of solar radiation, a variable supply of water and nutrients in the soil, a strong dependency of biochemical growth and development processes on ambient temperatures, agricultural practices, etc.

Phenology is the study of the timing of recurring natural phenomena. When applied to plants, it aims at determining the dates of remarkable events such as the start of growth, or the initiation of major developmental phases such as budding or flowering. In the context of this paper, the expression 'growing season' refers to the time period during which vegetation maintains any sort of activity (photosynthesis, redistribution of material resources through stem flow, etc.) above the latent or dormant period, which corresponds to the winter or dry season, depending on latitude and climate. This is somewhat of a misnomer, since vegetation characteristics such as leaf area index, chlorophyll concentration, biomass, etc., both increase and decrease during that time, but it follows common practice.

Different users or applications may require different criteria to determine the nature and timing of these critical events. For example, in the case of agricultural crops, the growing season is often defined as the period during which mean daily air temperatures remain above a given threshold, such as 5 °C for wheat or 10 °C for maize (Jones, 1983), or as the period between the last killing frost in the spring and the first killing frost in the subsequent winter, e.g., Griffiths (1966) or Trewartha (1968). In terrestrial carbon cycling studies, the critical events may be the start, end, and length of the period when the plants are net sinks of carbon, as determined by eddy correlation methods. Monitoring the seasonality of vegetation is thus crucial to account for the seasonality of the atmospheric CO_2 concentration (e.g., Keeling et al., 1996) and the terrestrial

* Corresponding author.
E-mail address: Michel.Verstraete@jrc.it (M.M. Verstraete).

0273-1177/$34.00 © 2007 COSPAR. Published by Elsevier Ltd. All rights reserved.
doi:10.1016/j.asr.2007.05.066

component of the carbon cycle (e.g., White et al., 1999; Hall et al., 2006).

At the same time, any requirement to document vegetation phenology over large areas will have to rely on remote sensing, even though these observations may only be indirectly related to the events or geophysical variables mentioned earlier. Advances in Earth observation techniques, especially from space-based platforms, as well as in radiation transfer theory and algorithm developments, have led to the operational generation of biogeophysical products that are particularly useful for such purposes (e.g., Justice et al., 1985). Numerous studies have previously been carried out to characterize vegetation phenology, and in particular growing seasons, on the basis of such observations. These investigations have generally exploited a vegetation index, which is deemed to represent the dynamic evolution of some vegetation property (see, for instance, Delbart et al., 2005, 2006; White and Nemani, 2006; Bradley et al., 2007; Kathuroju et al., 2007 and the references therein, amongst many others, for recent work in this field).

Although primarily designed to describe the evolution of plants in an agricultural context, growing seasons are applicable to all seasonally varying vegetated ecosystems. Synthetic information on the phenology of plants has been found useful in land cover classification (e.g., Hansen et al., 2000), the parameterization of land surface processes in climate models (e.g., Schulz et al., 2001) or carbon models (e.g., Knorr and Schulz, 2001). Since terrestrial vegetation partly controls the exchanges of carbon dioxide between land surfaces and the overlying atmosphere and exhibits significant sensitivity to weather and climate events, monitoring its evolution in space and time provides direct evidence about this surface–atmosphere coupling and its implications (Cayan et al., 2001). The characteristics of growing seasons are also of direct relevance to global change science, in particular for the monitoring of vegetation and the assessment of net primary production (Nemani et al., 2003).

While it may be difficult to generalize local, ground-based approaches – any reference to a freezing event, to be recorded from sheltered thermometers, may not be applicable wherever such equipment is unavailable or in regions where it never freezes, it is useful to distinguish between two different issues: the detection of key events in a time series, using appropriate statistical tools, and relating these events to the specific needs of a particular application.

The prime objective of this study is to define and evaluate a method to determine key characteristics of the phenology of terrestrial environments on the basis of a statistical analysis of satellite remote sensing biophysical products in the solar spectral domain, the primary source of information, subject to two specific constraints, namely to be widely applicable, and without requiring expert knowledge or operator intervention. The first one implies being able to detect key phenological characteristics such as the start, end, and length of growing seasons for a range of ecosystems and vegetation types. The second means that the detection algorithm must be quite robust and able to deal with a variety of situations including missing values due to cloud obscurations, snow cover, or lack of seasonal solar illumination, possible outliers, etc., and not require ancillary information on the biome or species, soil characteristics or the evolution of local weather and climate variables.

2. Input data: the JRC-FAPAR product

In this paper, the Fraction of Absorbed Photosynthetically Active Radiation (FAPAR) has been chosen as the primary source of information on the seasonality of plant canopies, both because it is a physically based product directly related to ecological issues such as growth and development, carbon assimilation, etc., and because this particular biophysical variable is a typical Level-2 product that can now be reliably and accurately derived from data acquired by a variety of Earth observing instruments (Gobron et al., 2005a). In fact, a suite of algorithms to consistently derive FAPAR estimates from some of the most popular space-based instruments (Gobron et al., 2000), including, for instance, SeaWiFS (Gobron et al., 2001), MERIS (Gobron et al., 2004), or MODIS (Gobron et al., 2006b) has been developed, and an extensive archive of FAPAR products based on the SeaWiFS data has been generated and made publicly available on-line.[1] Considerable efforts have also been spent in verifying the compatibility of these products, both between themselves and with field measurements (e.g., Gobron et al., 2006a, 2007).

All results reported below were obtained from an analysis of SeaWiFS FAPAR decadal products generated at the Joint Research Centre (JRC), though the same approach could be used to process anyone of a number of such products. Daily FAPAR products are combined for successive 10-day periods, except that the last period of each month may contain from 8 to 11 days, so that the records remain synchronized with the calendar months. Detailed instructions to generate these composited decadal products are available in the form of an Algorithm Theoretical Basis Document (Pinty et al., 2002).

3. Methodology

For simplicity, the following methodological discussion focuses on the analysis of decadal FAPAR time series for single sites. The seasonal evolution of this biogeophysical variable for a typical agricultural site (in this case, Bondville, IL, USA) is exhibited in Fig. 1 for a limited series of 4 years. The yearly growth and senescence phases are clearly visible, and the aim is to design a numerical algorithm that will objectively and automatically detect the start of the growth and the end of the senescence periods. The method proceeds through three main phases: the first

[1] http://fapar.jrc.ec.europa.eu/.

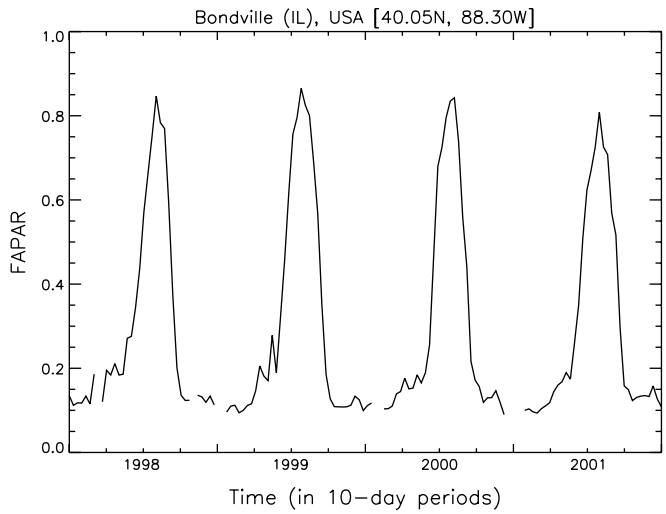

Fig. 1. Evolution of FAPAR for an agricultural site, here Bondville, IL, USA. The seasonality of the signal is clearly visible in this typical time series.

one aims at deriving gross statistical properties and assessing the likely number of growing seasons per year. During the second phase, an S-shaped mathematical model is fitted through subsets of the data corresponding to successive positions of a moving window. In the third phase, the results obtained earlier are analyzed to determine the dates of key phenological events.

3.1. Description of Phase 1: pre-processing

The main purpose of the pre-processing phase is to derive from the FAPAR record itself preliminary information on the likelihood of finding 0, 1, or 2 growing seasons per period of 12 consecutive months.

Determining the expected number of growing seasons per year is achieved by computing the autocorrelation function for all time lags up to 45 decadal periods. Lags somewhat longer than a full year (36 decades) are included to ensure that the yearly cycle is properly recognized. This autocorrelogram is further smoothed with a 5-point moving average filter to remove any spurious fluctuations resulting from the variable number of correlation pairs at various lags (this results from the presence of missing values), and the shape of that smoothed autocorrelogram is analyzed to count the number of local maxima: if only one is found, typically at lag 0, the autocorrelogram exhibits progressively decreasing values at longer lags and the FAPAR record does not exhibit any seasonal variation, so that no growing seasons are expected. One or two growing seasons are expected if the autocorrelogram exhibits two or three local maxima, respectively.

3.2. Description of Phase 2: model fitting

During Phase 2, a moving window is successively displaced, one decade at a time, over the entire time series, and the S-shaped model is optimally fitted to the valid (i.e., non-missing) FAPAR values available within that window. Various functions could be (and have been) used for that purpose, including polynomials (e.g., Bradley et al., 2007) and sigmoids (e.g., Ahl et al., 2006; Fisher et al., 2007). We have chosen to use the following parametric sigmoid model:

$$y = \frac{a}{1 + \exp(-b(x - c))} + d \tag{1}$$

In this case, a defines the total amplitude of the curve, b sets the sign and strength of the slope of the curve, c specifies the horizontal offset, and d controls the vertical offset of the curve. A non-linear fitting procedure is used to estimate the most likely values of the model parameters a, b, c, and d, given the valid FAPAR values in the specified moving window.

Such a routine typically requires some reasonable initial guess values for the four model parameters, and some care needs to be given to their specification, so as to minimize the time spent to iteratively search for the solution and to ensure a good accuracy (e.g., Press et al., 1992; Verstraete et al., 2000). Here, we set these initial values as follows:

- a is calculated as the difference between the maximum and the minimum FAPAR values within the moving window,
- b is empirically estimated as 20 times the slope of a linear fit through the valid FAPAR values within the window,
- c is set to the time index corresponding to the middle of the moving window, and
- d is set to the minimum valid FAPAR value within the moving window.

The moving window itself must be long enough to contain, on average, a sufficient number of points for the non-linear fitting procedure to be able to work. Since the sigmoid model uses four parameters, a minimum of 5 decades would be required. On the other hand, it would not make sense to use a window that is much larger than the typical length of the growing or of the senescence phase for the vegetation. Reasonable values for this parameter thus range from about 7 to 12, and a 10-decade long (`WinLen` = 10) window has empirically been found to be adequate.

At the end of this phase, the optimal values of the four model parameters are available for each possible position of the moving window within the entire time series. These series can themselves contain gaps, as the sigmoid model fitting procedure cannot work if there are too few FAPAR values within the moving window: this may happen in the winter at high latitude, for instance, and examples will be shown later.

3.3. Description of Phase 3: characterizing the phenology

The results accumulated in Phases 1 and 2 are analyzed in Phase 3 to determine the start, end, and length of the

growing seasons. The first issue is to detect the start of the initial growing season, given that (1) FAPAR records are expected to be available for full calendar years (January to December, possibly including an arbitrary number of missing values at the start of the first year), (2) there is no causal relation between the start or end of a growing season and the calendar years (in other words, one cannot assume that any particular calendar year contains a complete growing season), and (3) there is no a priori relation either between the start of remote sensing records and the start of growing seasons at any arbitrary location.

To address this problem, the FAPAR time series is analyzed sequentially from the start, using the results of Phase 1, to (1) locate the first time a valid value lower than a predefined threshold is encountered, (2) advance further in time as long as FAPAR values remain lower than this threshold, and (3) identify the first time when an FAPAR value raises above that threshold, which is currently set at the median of the entire FAPAR distribution. Since this event is likely within the rapid growth of the first documented growing season, the search for that first growing season will be confined within an appropriate sub-period, typically from 10 decades before to 20 decades after the current location in the time series.

Within that limited time sub-period, the algorithm analyzes the sigmoid model fit results retrieved during Phase 2 to identify the position of the moving window for which the amplitude model parameter a is maximum and the slope model parameter b is positive. The growing season is deemed to start on the first decade of that moving window. Similarly, the end of that first growing season is taken to be the last decade of the moving window for which the corresponding amplitude model parameter is maximum while the slope is negative.

The rest of the FAPAR time series is processed in the same way, each time looking for a start or and end event within a period that initiates with the last event found. If the end of the entire FAPAR record is reached before the last growing season is completed, the characteristics of that season are not reported. Once the start and end events are known for each growing season, it is a trivial matter to estimate the length of the corresponding seasons.

4. Results

The algorithm described above has been applied to analyze time series of FAPAR products for various sites located in different biomes. The first example (see Fig. 2) involves the well-behaved time series for the agricultural site in Bondville, IL, USA, mentioned earlier, which is also one of the 'BigFoot' validation sites for remote sensing products.[2] The main crops grown on that site include corn and soybean, in rotation.

The corresponding numerical values are reported in Table 1. It can be seen that the growing seasons are fairly stable, but that there are nevertheless small year-to-year variations.

The second example (Fig. 3) involves analyzing the FAPAR time series for Braschaat, Belgium, one of the CarboEurope field study sites.[3]

This is a mixed forest ecosystem with less regular seasonal cycles (higher FAPAR variability during the growing seasons and more dispersion in length) than the previous fully controlled agricultural site. The corresponding statistics for that site are reported in Table 2. Note that the widespread drought that afflicted much of Western Europe in 2003 (see, e.g., Gobron et al., 2005b) did not seem to impact the growing season length for this mixed forest environment: if anything, the active season in 2003 seems somewhat longer (270 days) than the average (251 days) for the available record. This is still well within the typical values encountered before and after, and in any case the maximum FAPAR value reached is somewhat lower than in other years.

A third example is provided by the BOREAS Northern Study Area (NSA) site,[4] covered primarily with black spruce, scattered birch and some stands of jack pine. Fig. 4 shows the time series and model fits, while Table 3 provides the corresponding numerical values.

The effect of missing data during the winter months due to prevalent cloudiness and snow on the fitting of the sigmoid model can clearly be observed: in the absence of constraints, small variations in FAPAR values at the start or at the end of the observed period may occasionally result in model parameter sets that would imply large variations during the unobserved period. This, however, does not impact the detection of start and end events because the software procedure ignores any and all simulated values that do not correspond to a measured and valid value.

Fig. 5 shows the results obtained for a site located even further north, namely Flakaliden, Sweden, around 64°N.

In this case, satellite observations may not be collected during the winter due to lack of light, and some snow cover may also remain on the ground in late spring or appear in early autumn: the FAPAR generating algorithm will detect and flag such cases, and will not report an FAPAR value, because it would be highly unreliable. The growing season algorithm is thus left with a rather truncated series and will report start and end growing season events that generally correspond to the period when FAPAR can be reliably estimated. The corresponding statistics are reported in Table 4.

The results for two other sites are exhibited next to show how this algorithm performs in different biomes. The first one is for the CarboAfrica site of Skukuza in South Africa. Fig. 6 shows that this site is subject to significant year-to-year variations, both in amplitude and shape of the FAPAR seasonal signal.

[2] http://www-eosdis.ornl.gov/BIGFOOT_VAL/bigfoot.html.

[3] http://www.bgc-jena.mpg.de/public/carboeur/sites/index_s.html.

[4] http://www-eosdis.ornl.gov/BOREAS/bhs/Sites/NSA.html.

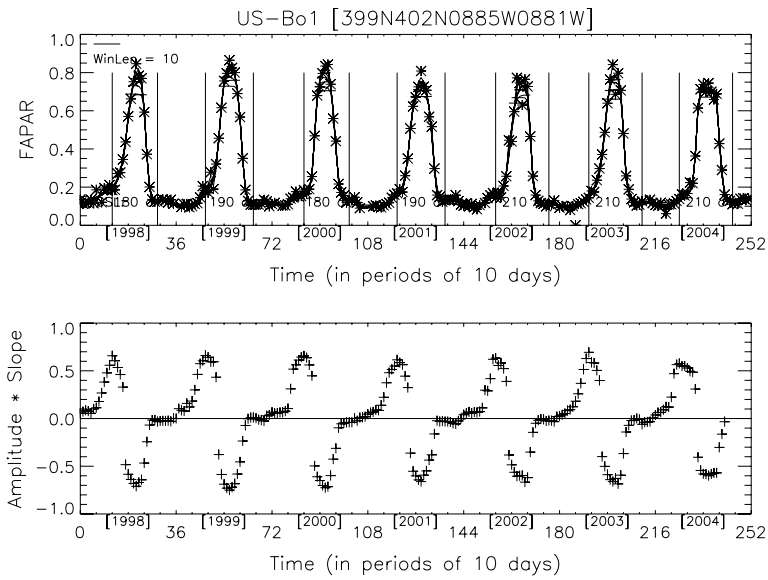

Fig. 2. Top panel: FAPAR time series (star symbols) for Bondville (IL), USA, with the sigmoids for each moving window superimposed. The length of the moving window (here, `WinLen` = 10 decades) is exhibited in the top left corner of this panel. Bottom panel: product of the amplitude and slope parameters. The growing seasons are deemed to start when this latter curve peaks, and to stop `WinLen` decades after the curve reaches its minimum annual value. These start and end events are reported in the top panel as vertical bars, and the lengths of each of the growing seasons are also indicated in days.

Table 1
Start (S), end (E), and length (L) of growing seasons for Bondville, IL, USA

	1998	1999	2000	2001	2002	2003	2004
S	12	12	13	12	13	12	10
	[111–120]	[111–120]	[121–130]	[111–120]	[121–130]	[111–120]	[91–100]
E	29	30	30	30	33	32	30
	[284–293]	[294–304]	[294–304]	[294–304]	[325–334]	[315–324]	[294–304]
L	18	19	18	19	21	21	21

All values are in decades, since the start of the indicated year in the case of dates. [Numbers in brackets indicate the corresponding 'day of the year'.]

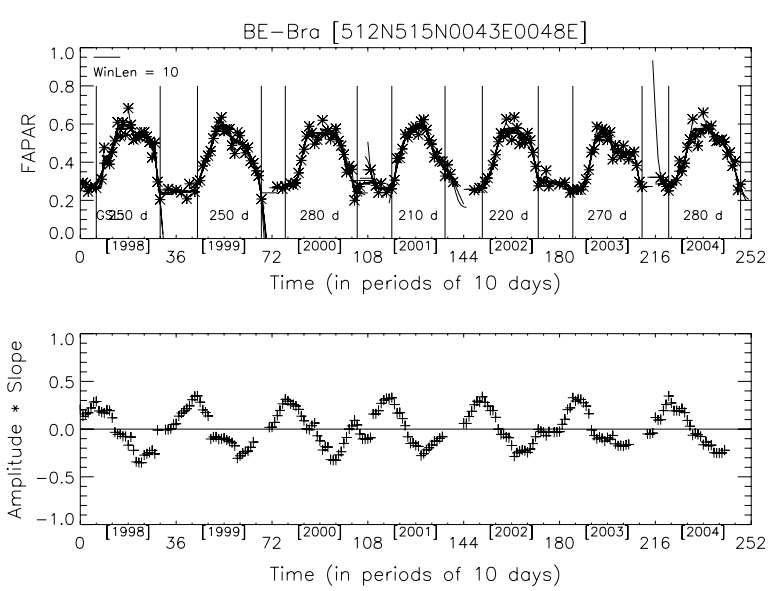

Fig. 3. Same as for Fig. 2, but for Braschaat, Belgium. Note the irregular yearly seasonal growing seasons and the occasional lack of data in the winter.

Table 2
Start (S), end (E), and length (L) of growing seasons for Braschaat, Belgium

	1998	1999	2000	2001	2002	2003	2004
S	6	9	6	10	8	6	6
	[52–59]	[80–90]	[52–59]	[91–100]	[70–79]	[52–59]	[52–59]
E	30	33	33	30	29	32	33
	[294–304]	[325–334]	[325–334]	[294–304]	[284–293]	[315–324]	[325–334]
L	25	25	28	21	22	27	28

All values are in decades, since the start of the indicated year in the case of dates. [Numbers in brackets indicate the corresponding 'day of the year'.]

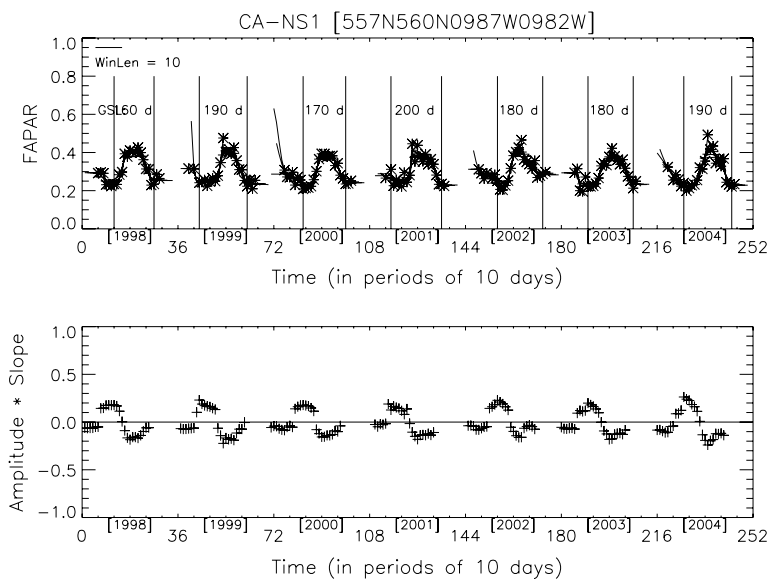

Fig. 4. Same as for Fig. 2, but for the Boreas NSA site in Canada.

Table 3
Start (S), end (E), and length (L) of growing seasons for the Northern Boreas Study Area (NSA) site in Canada

	1998	1999	2000	2001	2002	2003	2004
S	12	9	12	9	13	11	11
	[111–120]	[80–90]	[111–120]	[80–90]	[121–130]	[101–110]	[101–110]
E	27	27	28	28	30	28	29
	[264–273]	[264–273]	[274–283]	[274–283]	[294–304]	[274–283]	[284–293]
L	16	19	17	20	18	18	19

All values are in decades, since the start of the indicated year in the case of dates. [Numbers in brackets indicate the corresponding 'day of the year'.]

Table 5 exhibits the corresponding statistics. Note that these growing seasons span consecutive calendar years because this site is in the Southern Hemisphere. All dates are provided in decades from the start of the relevant 2 years period.

Finally, a site selected within a semi-arid zone of China (Fig. 7) demonstrates that small but systematic variations can be detected as long as the seasonal variations exceed the noise in the data. The corresponding statistics are reported in Table 6.

5. Sensitivity of the results to the moving window length

The approach described above requires very few assumptions, as it does not rely on any a priori knowledge about the type of biome observed or about the nature of the most important limiting factors or constraints on plant growth. Nevertheless, it is useful to document the sensitivity of the results to the length of the moving window period, which has been empirically set to 10 decades in all examples shown earlier. Table 7 shows how the dates of the start and end of the growing seasons vary as a function of the selected moving window length, for the agricultural site of Bondville.

It can be seen that the dates of the start and end events do vary by about a decade or so with each increase or decrease of the moving window length by one decade within that range. That longer moving windows are associated with somewhat earlier starts and later ends is fully expected, since the sigmoid fit that best matches the growth

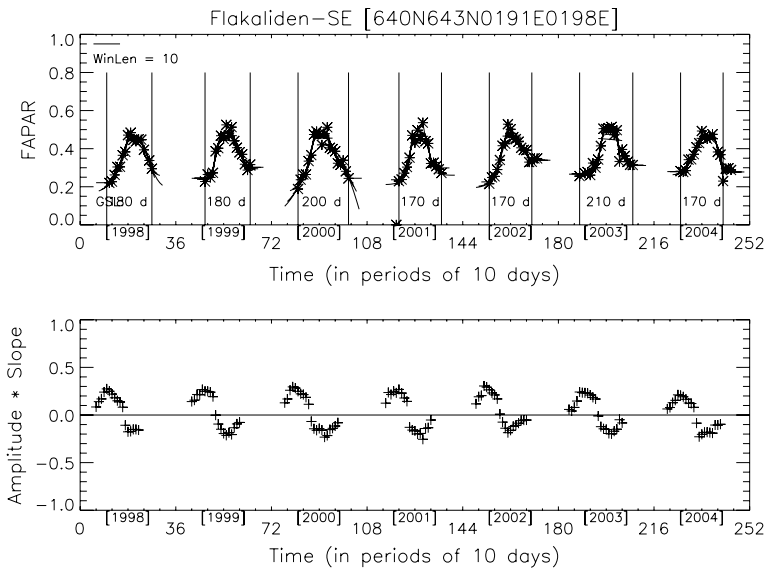

Fig. 5. Same as for Fig. 2, but for the Flakaliden site in Sweden.

Table 4
Start (S), end (E), and length (L) of growing seasons for the Flakaliden site in Sweden

	1998	1999	2000	2001	2002	2003	2004
S	10	12	11	13	11	9	11
	[91–100]	[111–120]	[101–110]	[121–130]	[101–110]	[80–90]	[101–110]
E	27	29	30	29	27	29	27
	[264–273]	[284–293]	[294–304]	[284–293]	[264–273]	[294–304]	[264–273]
L	18	18	20	17	17	21	17

All values are in decades, since the start of the indicated year in the case of dates. [Numbers in brackets indicate the corresponding 'day of the year'.]

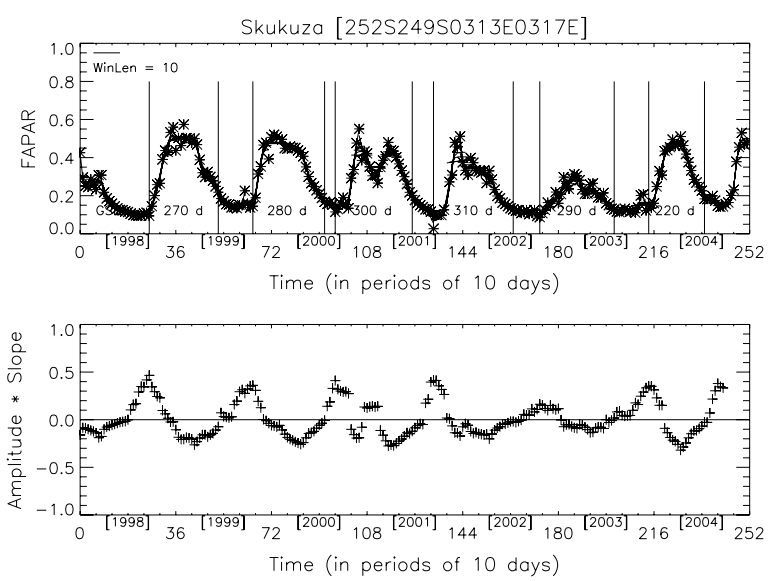

Fig. 6. Same as for Fig. 2, but for the Skukuza site in South Africa.

and senescence phases will be essentially locked at the same places in the time series, and it is numerically 'easier' to extend the sigmoid fit in the low variability period between the growing seasons than in the highly variable period near the maximum.

Selecting a short value for the moving window length may limit the applicability of the method whenever the frequency of missing values increases. Also, if the FAPAR time series includes occasional outliers, a short moving window length may result in the sigmoid model attempting

Table 5
Start (S), end (E), and length (L) of growing seasons for the Skukuza site in South Africa

	1998–99	1999–00	2000–01	2001–02	2002–03	2003–04
S	26	30	25	26	30	35
	[254–263]	[294–304]	[244–253]	[254–263]	[294–304]	[345–354]
E	52	57	54	56	58	56
(*)	[152–161]	[202–212]	[172–181]	[192–201]	[213–222]	[192–201]
L	27	28	30	31	29	22

All values are in decades, since the start of the indicated period in the case of dates. [Numbers in brackets indicate the corresponding 'day of the year'.] A star (*) indicates a date in the second year of the indicated period.

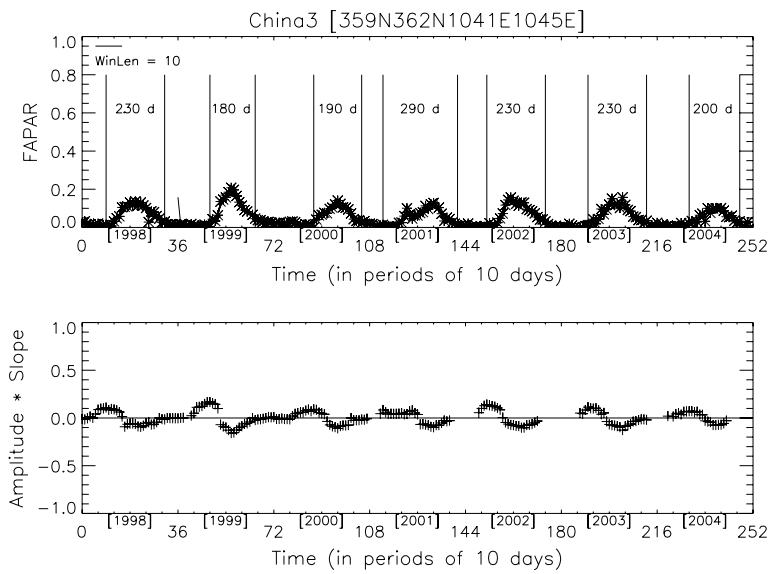

Fig. 7. Same as for Fig. 2, but for a semi-arid site in China.

Table 6
Start (S), end (E), and length (L) of growing seasons for a semi-arid site in China

	1998	1999	2000	2001	2002	2003	2004
S	9	13	16	6	9	11	13
	[80–90]	[121–130]	[152–161]	[52–59]	[80–90]	[101–110]	[121–130]
E	31	30	34	34	31	33	32
	[305–314]	[294–304]	[335–344]	[335–344]	[305–314]	[325–334]	[315–324]
L	23	18	19	29	23	23	20

All values are in decades, since the start of the indicated year in the case of dates. [Numbers in brackets indicate the corresponding 'day of the year'.]

Table 7
Sensitivity of the results to moving window length (`WinLen`), for Bondville, USA

`WinLen`		1998	1999	2000	2001	2002	2003	2004
7	S	15	15	15	15	15	15	13
	E	27	28	28	27	30	29	30
8	S	14	15	15	14	15	14	12
	E	28	28	29	28	31	30	28
9	S	13	13	14	13	13	13	11
	E	29	29	29	29	32	31	29
10	S	12	12	13	12	13	12	10
	E	29	30	30	30	33	32	30
11	S	11	11	12	11	12	11	9
	E	31	31	31	31	34	32	31
12	S	10	10	11	10	11	10	8
	E	32	32	32	32	34	32	32

All numbers are in units of decades since the start of the record (1 January 1998).

to fit small variations, possibly leading to the detection of spurious start or end events. Conversely, setting the window length closer to the largest meaningful value (half a year or 18 decades) results in a lack of sensitivity to year-to-year changes. A moving window length of 10 decades has been found satisfactory in most cases studied here.

6. Comparison with other approaches

As noted earlier, various authors have proposed a wide range of methods to assess plant phenology. It is thus interesting to compare the results obtained on the same sites and for the same years, although that apparently simple goal turns out to be rather uneasy to achieve in practice, as will be seen shortly.

Direct comparisons with field observations are always going to be problematic because the latter are relative to small areas (from 1 to 100 square meters) compared to the 'pixel' surface observed from space, which is typically a few hectares to a few square kilometers. However, the main difficulty has to do with the fact that there is no general agreement about what defines the start of a growing season. For these reasons, it is deemed more appropriate to study the coherency between remote sensing products.

The first comparison refers to the results published by Bradley et al. (2007), who estimated the 'onset of greenness' for three specific sites on the basis of NDVI records extracted from the NOAA AVHRR Pathfinder programme. The three biomes are identified as 'Montane' (39.3000°N, 117.1378°W), 'Sagebrush' (39.4753°N, 116.61°W), and 'Cheatgrass' (40.1647°N, 117.1°W), respectively, and are located in the US Great Basin. The dates of the start of the growing seasons for the same locations and for those years for which the JRC-FAPAR product was available have been estimated. Table 8 shows how the timing of these events compare according to these two methods.

The values reported in the columns 'Bradley' were derived from the data used to generate Fig. 6 in Bradley et al. (2007) (personal communication), converted into day ranges because their original data were weekly composites (nominal value plus and minus 3 days). The ranges reported in the columns 'this study' refer to the first and last day of the decade pointing to the start of the growing season.

Differences between these dates are obviously resulting from the rather different approaches used to characterize these phenological events: Bradley et al. define the 'onset of greenness' as the date when the NDVI value reaches half its maximum value, while our 'start of the growing season' generally refers to the timing of the earliest observed rise of the FAPAR signal itself, above the values typically experienced between growing seasons (e.g., during the winter). It is thus expected that our dates for the start of growing seasons should be rather much sooner than the dates of the onset of greening. Interestingly, inspecting Fig. 4 of Bradley et al. (2007), it can be seen that even according to their NDVI profile for 1998, the values of that index actually start increasing within the first few weeks of the year for Cheatgrass and after 'day of the year' 100 for the Montane ecosystem. In the case of Sagebrush, the seasonal cycles are rather small or inexistent, whether in the NDVI or in the FAPAR signals. All in all, these results are not inconsistent, though difficult to compare head-on.

Although much research has focused on the use of remote sensing techniques in the solar spectral domain to document the phenology of vegetation, similar advances have been proposed in the microwave domain (e.g., Kimball et al., 2004). In this second case, we compare our results with those of Min and Lin (2006), obtained using the Emissivity Difference Vegetation Index (EDVI) computed from the 19.4 and 37.0 GHz channels retrieved from the SSM/I instrument for the Harvard Forest LTER site (42.5°N, 72.2°W). They published results for years 1999 and 2000 only, but these are included in the JRC-FAPAR database.

Application of the algorithm described above to the JRC-FAPAR record from the same location and for years 1999 and 2000 identifies the growing seasons as starting in decade 8 in both years. Within our scheme, this corresponds to the period 11–20 March or to 'days of the year' in the range 70–79. This is about 50 days or so earlier than the 'spring onset' dates reported by Min and Lin (2006), which ranges from days of the year 122–132 in these same 2 years. However, here again, a close look at the methodology reveals that, in this latter case, spring onset is deemed to occur on the date of the maximum second derivative of the microwave emissivity difference vegetation index. This event is better associated with the timing of the fastest growth than the start of an observable change in FAPAR. These results are in fact fully compatible with the approach proposed here, because the inflexion point of the sigmoid would occur mid-way through the moving window period, i.e., 5 decades after the start of the growing season as defined here.

Table 8
Dates (day of year) of the 'onset of greenness' and start of the growing season, according to the results of Bradley et al. (2007) and this study

	1998		1999		2000	
	Bradley	This study	Bradley	This study	Bradley	This study
Montane	161–167	111–120	155–161	80–90	134–140	80–90
Sagebrush	125–131	60–69	114–120	60–69	119–125	80–90
Cheatgrass	118–124	1–10	93–99	1–10	120–126	32–40

7. Conclusion

In summary, there are no currently accepted standards to define the start and end of growing seasons, in large part because each application may have specific needs, which are often addressed through different methodologies. Any attempt to understand why or how vegetation evolves as it does at a specific location must analyze in detail the limiting factors that control the growth and development of plants. These findings, while highly relevant for the particular species under study, remain circumstantial and hard to generalize, as relations adequate for agriculture may not be applicable to forests, for instance.

On the other hand, a phenomenological approach based on remote sensing products such as proposed in this paper leads to a spatially and temporally coherent characterization of vegetation phenology. While not providing evidence to support causal relationships, the method relies only on the observed evolution of the vegetation itself whenever and wherever it occurs, and is therefore automatically applicable everywhere and all the time, independently of the biome, climate or other local conditions. This is particularly useful in studies of relative variations in space or time, or when evidence from the field is lacking or difficult to acquire.

Relying on the JRC-FAPAR product, this analysis was able to focus on the statistical properties of the time series, without concerns for the instrumental, environmental or observational side effects that often affect traditional sources such as vegetation indices. Also, the tools described here have been shown to be, within reasonable limits, rather insensitive to the presence of outliers or missing values.

Future work will focus on a more detailed characterization of vegetation phenology from space, on applications to large areas and on evaluating possible relations between these statistical indicators and generic properties of the vegetation, such as biomass accumulation, gross primary productivity or net ecosystem exchange of carbon with the atmosphere.

References

Ahl, D.E., Gower, S.T., Burrows, S.N., Shabanov, N.V., Myneni, R.B., Knyazikhin, Y. Monitoring spring canopy phenology of a deciduous broadleaf forest using MODIS. Remote Sensing of Environment 104, 88–95, doi:10.1016/j.rse.2006.05.003, 2006.

Bradley, B.A., Jacob, R.W., Hermance, J.F., Mustard, J.F. A curve fitting procedure to derive inter-annual phenologies from time series of noisy satellite NDVI data. Remote Sensing of Environment 106, 137–145, doi:10.1016/j.rse.2006.08.002, 2007.

Cayan, D., Kammerdiener, S.A., Dettinger, M.D., Caprio, J.M., Peterson, D.H. Changes in the onset of spring in the western United States. Bulletin of the American Meteorological Society 82, 399–415, 2001.

Delbart, N., Kergoat, T., Le Toan, L., Lhermite, T.J., Picard, G. Determination of phenological dates in boreal regions using normalized difference water index. Remote Sensing of Environment 97, 26–38, doi:10.1016/j.rse.2005.03.011, 2005.

Delbart, N., Le Toan, T., Kergoat, L., Fedotova, V. Remote sensing of spring phenology in boreal regions: a free of snow-effect method using NOAA-AVHRR and SPOT-VGT data (1982–2004). Remote Sensing of Environment 101, 52–62, doi:10.1016/j.rse.2005.11.012, 2006.

Fisher, J.I., Richardson, A.D., Mustard, J.F. Phenology from surface meteorology does not capture satellite-based greenup estimations. Global Change Biology 13, 1–15, doi:10.1111/j.1365-2486.2006.01311.x, 2007.

Gobron, N., Pinty, B., Verstraete, M.M., Widlowski, J.-L. Advanced vegetation indices optimized for up-coming sensors: design, performance and applications. IEEE Transactions on Geoscience and Remote Sensing 38, 2489–2505, 2000.

Gobron, N., Mélin, F., Pinty, B., Verstraete, M.M., Widlowski, J.-L., Bucini, G. A global vegetation index for SeaWiFS: design and applications, in: Beniston, M., Verstraete, M.M. (Eds.), Remote Sensing and Climate Modeling: Synergies and Limitations. Kluwer Academic Publishers, Dordrecht, pp. 5–21, 2001.

Gobron, N., Aussedat, O., Pinty, B., Taberner, M., Verstraete, M.M., Medium Resolution Imaging Spectrometer (MERIS) – Level 2 Land Surface Products – Algorithm Theoretical Basis Document, Revision 3.0. Institute for Environment and Sustainability, EUR Report No. 21387 EN, 20 pp., 2004.

Gobron, N., Pinty, B., Taberner, M., Mélin, F., Verstraete, M.M., Widlowski, J.-L. Monitoring the photosynthetic activity of vegetation from remote sensing data. Advances in Space Research 38, 2196–2202, doi:10.1016/j.asr.2003.07.079, 2005a.

Gobron, N., Pinty, B., Mélin, F., Taberner, M., Verstraete, M.M., Belward, A., Lavergne, T., Widlowski, J.-L. The state vegetation in Europe following the 2003 drought. International Journal Remote Sensing Letters 26, 2013–2020, 2005b.

Gobron, N., Pinty, B., Aussedat, O., Chen, J., Cohen, W.B., Fensholt, R., Gond, V., Hummerich, K.F., Lavergne, T., Mélin, F., Privette, J.L., Sandholt, I., Taberner, M., Turner, D.P., Verstraete, M.M., Widlowski, J.-L. Evaluation of FAPAR products for different canopy radiation transfer regimes: methodology and results using Joint Research Center products derived from SeaWiFS against ground-based estimations. Journal of Geophysical Research 111, D13110, doi:10.1029/2005JD006511, 2006a.

Gobron, N., Aussedat, O., Pinty, B., MODerate Resolution Imaging Spectroradiometer (MODIS) – JRC-FAPAR at 250 m Algorithm Theoretical Basis Document. European Commission, DG Joint Research Centre, Institute for Environment and Sustainability, EUR Report No. 22279 EN, pp. 1–31, 2006.

Gobron, N., Pinty, B., Mélin, F., Taberner, M., Verstraete, M.M., Robustelli, M., Widlowski, J.-L. Evaluation of the MERIS/ENVISAT FAPAR product. Advances in Space Research 39, 105–115, doi:10.1016/j.asr.2006.02.048, 2007.

Griffiths, J.F. Applied Climatology: An Introduction. Oxford University Press (118 pp.), 1966.

Hall, F., Masek, J.G., Collatz, G.J. Evaluation of ISLSCP initiative II FASIR and GIMMS NDVI products and implications for carbon cycle science. Journal of Geophysical Research 111, D22S08, doi:10.1029/2006JD007438, 2006.

Hansen, M.C., Defries, R.S., Townshend, J.R.G., Sohlberg, R. Global land cover classification at 1 km spatial resolution using a classification tree approach. International Journal of Remote Sensing 21, 1331–1364, 2000.

Jones, H.G. Plants and Microclimate. Cambridge University Press (323 pp.), 1983.

Justice, C.O., Townshend, J.R.G., Holben, B.N., Tucker, C.J. Analysis of the phenology of global vegetation using meteorological satellite data. International Journal of Remote Sensing 6, 1271–1318, 1985.

Kathuroju, N., White, M.A., Symanzik, J., Schwartz, M.D., Powell, J.A., Nemani, R.R. On the use of the advanced very high resolution radiometer for development of prognostic land surface phenology models. Ecological Modelling 201, 144–156, doi:10.1016/j.ecolmodel.2006.09.011, 2007.

Keeling, C.D., Chin, J.F.S., Whorf, T.P. Increased activity of northern hemispheric vegetation inferred from atmospheric CO_2 measurements. Nature 382, 146–149, 1996.

Kimball, J.S., McDonald, K.C., Running, S.W., Frolking, S.E. Satellite radar remote sensing of seasonal growing seasons for boreal and subalpine evergreen forests. Remote Sensing of Environment 90, 243–258, doi:10.1016/j.rse.2004.01.002, 2004.

Knorr, W., Schulz, J.-P. Using satellite data assimilation to infer global soil moisture status and vegetation feedback to climate, in: Beniston, M., Verstraete, M.M. (Eds.), Remote Sensing and Climate Modeling: Synergies and Limitations, Advances in Global Change Research series, vol. 7. Kluwer Academic Publishers, Dordrecht, The Netherlands, pp. 273–306 (ISBN 0-7923-6801-0), 2001.

Min, Q., Lin, B. Determination of spring onset and growing season leaf development using satellite measurements. Remote Sensing of Environment 104, 96–102, doi:10.1016/j.rse.2006.05.006, 2006.

Nemani, R.R., Keeling, C.D., Hashimoto, H., Jolly, W.M., Piper, S.C., Tucker, C.J., Myneni, R.B., Running, S. Climate-driven increases in global terrestrial net primary production from 1982 to 1999. Science 300, 1560–1563, 2003.

Pinty, B., Gobron, N., Mélin, F., Verstraete, M.M., Time Composite Algorithm Theoretical Basis Document. Institute for Environment and Sustainability, EUR Report No. 20150 EN, 8 pp., 2002.

Press, W.H., Teukolsky, S.A., Vetterling, W.T., Flannery, B.P., second edNumerical Recipes in FORTRAN Cambridge University Press (ISBN 0-521-43064-X), 1992.

Schulz, J.-P., Dümenil, L., Polcher, J.A.N. On the land surface–atmosphere coupling and its impact in a single-column atmospheric model. Journal of Applied Meteorology 40, 642–663, 2001.

Trewartha, G.T. An Introduction to Climate. McGraw-Hill, New York (ISBN 07-065148-5), 1968.

Verstraete, M.M., Pinty, B. Environmental information extraction from satellite remote sensing data, in: Kasibhatla, P. et al. (Eds.), Inverse Methods in Global Biogeochemical Cycles, Geophysical Monograph 114. American Geophysical Union, pp. 125–137 (ISBN 0-87590-097-6), 2000.

White, M.A., Running, S.W., Thornton, P.E. The impact of growing-season length variability on carbon assimilation and evapotranspiration over 88 years in the eastern US deciduous forest. International Journal of Biometeorology 42, 139–145, 1999.

White, M.A., Nemani, R.R. Real-time monitoring and short-term forecasting of land surface phenology. Remote Sensing of Environment 104, 43–49, doi:10.1016/j.rse.2006.04.014, 2006.